Active rotor coning for a 25 MW downwind offshore wind turbine

Chao (Chris) Qin [1], Eric Loth [1], Daniel S. Zalkind [2], Lucy Y. Pao [3], Shulong Yao [4], D. Todd Griffith [4], Michael S. Selig [5], Rick Damiani [6]

[1] *Department of Mechanical and Aerospace Engineering, University of Virginia, Charlottesville, VA 22904, USA*

[2] *National Wind Technology Center, National Renewable Energy Laboratory (NREL), Arvada, CO 80007, USA*

[3] *Department of Electrical, Computer, and Energy Engineering, University of Colorado Boulder, Boulder, CO 80309, USA*

[4] *Department of Mechanical Engineering, University of Texas at Dallas, Richardson, TX 75080, USA*

[5] *Department of Aerospace Engineering, University of Illinois at Urbana-Champaign, Urbana, IL 61801, USA*

[6] *The Floating Wind Technology Company, LLC, Arvada, CO 80007, USA*

Author contact email: chrisqin@virginia.edu

Abstract. A two-bladed downwind turbine system was upscaled from 13.2 MW to 25 MW by redesigning aerodynamics, structures, and controls. In particular, three 25-MW rotors were developed, and the final version is a fully redesigned model of the original rotor. Despite their radically large sizes, it was found that these 25-MW turbine rotors satisfy this limited set of structural design drivers at the rated condition and that larger blade lengths are possible with conewise load-alignment. In addition, flapwise morphing (varying the cone angle with a wind-speed schedule) was investigated to minimize mean and fluctuating blade root bending loads using steady inflow proxies for the maximum and lifetime damage equivalent load moments. Compared to the fixed coned rotor case, morphing can provide an Annual Energy Production (AEP) increase of 6%, and the maximum blade root flapwise bending moment increases 21% (still under the constraint, i.e., 10% of the ultimate moments) as a trade-off. The resulting series of 25-MW rotors can be a valuable baseline for further development and assessment of ultra-large-scale wind turbines.

1. Introduction

Increasingly larger wind turbine rotors are anticipated due to increased power capture and reduced levelized cost of energy (LCOE). To address the mass and the blade design issues and respond to the challenges associated with extreme-scale wind turbine systems, a concept named the Segmented Ultralight Morphing Rotor (SUMR) was used to develop a set of 13.2-MW downwind blades [1, 2]. The SUMR-13 blades employed a load-aligned design with a downwind configuration and a coned rotor.

This is achieved by a combination of coning and aeroelastic deflection at a downwind angle (based on the combination of centrifugal, cantilever, and thrust forces) so that the net load forces align along the rotor blade. Simulation results show that this design can dramatically reduce the blade root flapwise bending moments, thereby allowing a 25% lower rotor mass while still maintaining the capture area and thus energy production [3]. In the present study, this novel rotor design using downwind load-alignment was further developed and increased in scale to allow an unprecedented 25 MW turbine.

A set of 25-MW rated two-bladed downwind rotors was investigated, starting from an upscaling of a 13.2-MW system in aerodynamics, structural redesign, and controller design. The load-aligned rotor configuration can dramatically reduce the cantilever loads and the stiffness requirement on the blades to allow management of rotor mass, aiming towards a reduction in LCOE.

2. Objectives

The main objective was to design a 25-MW two-bladed downwind rotor to withstand the critical design driving loads while dramatically increasing power capture and reducing LCOE. In particular, the focus was on increasing annual energy production (AEP) while managing the bending moments and damage equivalent loads (DEL) on the blade roots. The approach used starts with the upscaling a 13.2-MW downwind turbine to a 25-MW scale initial design (V1) based on scaling principles. This is followed by an updated design (V2) with redesigned aerodynamics, structures, and control systems. Finally, improvements were made with a final rotor re-design (V3) that considered new operating/control features. Critical aspects of these three designs are included in Qin *et al.* [4]. This design study evaluated the influence of active coning on flapwise and edgewise loads combined with the impact on AEP.

3. Methodology

3.1. Upscaling and Redesign Approaches

The initially developed 13.2-MW rotor downwind configuration (SUMR-13A) had two blades and a cone angle of 5° and a rated wind speed of 11.3 m/s [1]. A second and more advanced version (SUMR-13C) had a cone angle of 12.5° and longer blades, but same power rating [5]. The tower, drivetrain, and nacelle design were kept the same as the SNL-100-03 models [3], with blade lengths of 100 meters. The SUMR-13A and SUMR-13C baseline wind turbine models were upscaled to a pair of 25-MW designs (V1 and V2) using analytical scaling rules. Note that V1 is just a scaled-up version of SUMR-13A, and V2 is a scaled-up version of SUMR-13C with new chord and blade twist distributions. The scaling was based on the similarity method with the form of $N = N \cdot \eta^k$, where N is the parameter to be scaled, η is the scaling factor, and k is a power law factor that depends on the parameter to be scaled. Herein, the scaling factor is $\eta = L/L_0$, where L is the blade length, and L_0 indicates the original length of the baseline blade before scaling.

Note that scaling can be based on "fixed technology" (no design or topological changes) or based on "advancing technology" (design changes to accommodate the increasing scale and new technologies and designs). The former is based on classical beam mechanics theory, while the latter is based on empirical advances that have been demonstrated in the wind turbine industry. However, for the blade upscaling, the power-law factors need to be modified to be more realistic. The scaling for the rotor blades includes scaling for both flapwise and edgewise stiffness with resonance consideration and for the maximum pitching rate, which affects the capabilities of the control system. The power laws used for upscaling to 25 MW turbine components can be found in Qin *et al.* [4].

The V1 and V2 models were modified and upgraded to the V3 model with aerodynamic, structural, and control redesign, as shown in figure 1. (Due to the page limit, the discussion of V1 and V2 is not included in the present paper, but the details can be found in Qin *et al.* [4]) For the V3 model, the designed coning angle was increased to 22.5°, causing the blade length to further increase to 169 m, in order to maintain the same projected capture area. The structural design for the 25-MW V3 model satisfies the tip deflection requirement to avoid tower strikes for the extreme loading case. In addition,
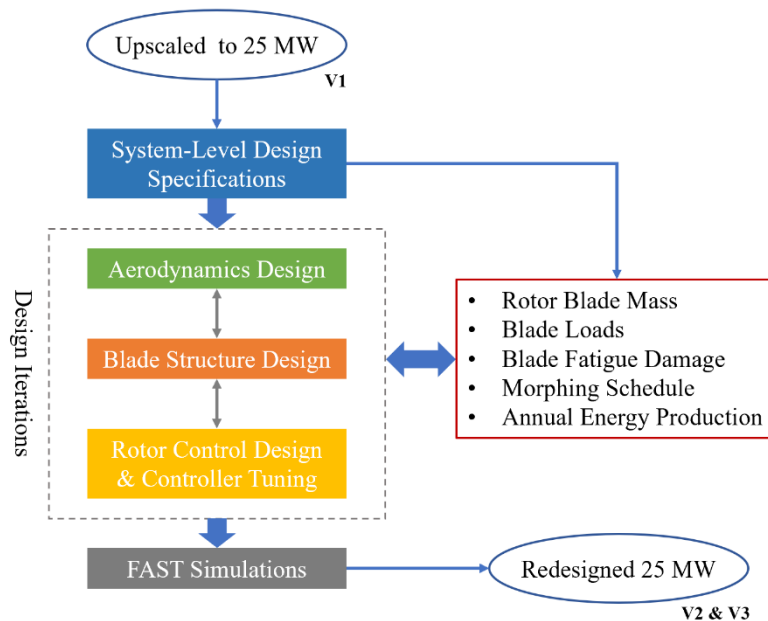
Figure 1. Rotor re-design process and design iterations among aerodynamics, structure, and control.

the design has a maximum safe strain for both flapwise and edgewise loading along the blade span for the extreme loading condition. The fatigue performance was checked by applying normal turbulence wind from cut-in to cut-out wind speeds, demonstrating a fatigue life greater than 20 years for both flapwise and edgewise directions. It was also found that the dynamics and flutter margin for the 25-MW V3 model meets the design requirements with acceptable flutter margin and no identified vibration issues. The structural design was in line with IEC conditions, the blade mass and stiffness distribution and the material/layouts were redesigned with corresponding aerodynamics designs. After each design iteration, when aerodynamic and structural models were updated, the controller was re-tuned using an automatic tuning algorithm [6], shown in figure 2. The below-rated torque controller was optimized for energy capture. The above-rated pitch controller was based on the NREL-5MW reference controller [7], a gain-scheduled, proportional-integral scheme. We optimized the proportional-integral gains of the pitch controller to minimize structural loading (and pitch actuation) [8], subject to a constraint on the maximum generator speed during turbulent simulations.
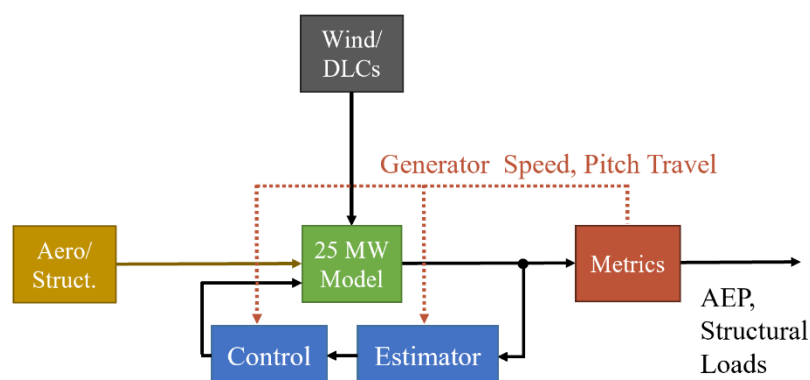

Figure 2. Aerodynamics, structural, and control designs are iterated to achieve a 25-MW wind turbine design that yields acceptable AEP, structural loads, generator speed regulation, and pitch travel, given wind and design load case (DLC) inputs.

3.2. Design Parameters and Simulation Tools

Aerodynamics design is performed using PROPID [9-11], which is an inverse rotor design tool that produces a rotor geometry based on desired aerodynamic performance. The desired performance specifications are set by the designer based on power, tip speed ratio, average wind speed, rated wind speed, and axial induction along the blade span. Structural design is performed using NuMAD [12]. The structural layup design in NuMAD allows for detailed material stacking and placement along the blade, and the frequency responses of the blades and the tower are calculated by BModes [13].

Aeroelastic simulations are implemented with a series of modules developed by NREL, whereby the core module is FAST (version 8) [14]. Different modules couple wind inflow with aerodynamic and elastic solvers that compute the structural loading on the wind turbine blades and tower. AeroDyn [15] was validated by blade element momentum method to predict the aerodynamic performance of such a highly coned rotor. Herein, the turbulent wind inputs are generated by TurbSim [16]. A MATLAB/Simulink interface is developed to process FAST simulations and perform closed-loop control with inputs of generator torque and pitch. Using the FAST results, fatigue is computed using MLife [17-18], which employs a rainflow counting algorithm to determine load cycles and extrapolates them over the lifetime of the wind turbine blades.

4. Results and Discussion

4.1. Rotors with Fixed Cone Angle and No Teeter

The V3 rotor design initially had a fixed cone angle of 22.5° and no teetering hub. We considered a steady and vertically sheared inflow and extracted mean and root-mean-square (RMS) values from the time-series outputs of aero-servo-elastic simulations. Note that the V3 blade length is 169 m, i.e., 12.7% longer than V1's 150 m length, while the blade mass is 25.3% larger (142.1 Mg vs. 113.4 Mg).

Table 1. V3 rotor results (no teeter) based on steady rated conditions (11.3 m/s).

Root **Flapwise** Bending Moment [MN-m]	MEAN	82.6
	RMS	29.2
	DEL	69.1
	ULT	1553
Root **Edgewise** Bending Moment [MN-m]	MEAN	18.2
	RMS	57.8
	DEL	131.8
	ULT	1527
Tip Deflection [m]	MEAN	12.9
	RMS	2.64
Clearance [m]	Undeflected	60.3

Due to the large coning angle, the V3 model operates closer to the natural flapwise equilibrium position (dictated by the balance of thrust and centrifugal loads) than the other models. As such, V3 simulations produced the smallest mean blade root flapwise bending moments (RFBMs) despite the longer and heavier blades. In addition, the higher coning of the V3 rotor yields a large tower-blade clearance to provide increased safety for large blade tip deformation. However, the higher coning angle model led to a lower maximum power coefficient (Cp). The maximum Cp of the V3 model obtained at rated condition was 0.42 as predicted by AeroDyn. As a reference, with no coning angle, the rotor simulations returned the expected maximum Cp value of 0.49. For the fatigue damage analysis for both flapwise and edgewise bending moments at the blade root, FAST outputs were used to calculate (via MLife) the average, root-mean-square, and the short-term damage equivalent load (denoted as

"MEAN", "RMS", and "DEL", respectively). The ultimate moment "ULT" was calculated based on the structural design. Exceeding "ULT" would lead to structural failure, and 10% of the ultimate moments (0.1*ULT) are set as the constraints on both maximum bending moments and accumulated damage (i.e., lifetime DEL) [1, 2]. The V3 results are shown in table 1.

4.2. Rotors with Morphing Schedule

The approach to reducing loads is to employ a variable coning angle through a morphing schedule as a function of the mean wind speed [19]. The objective of such a morphing schedule is for the rotor to have low coning below the rated condition so as to extract more energy (by flattening the rotor to increase swept area), and higher coning above the rated wind speed and in extreme conditions reduced mean flapwise bending moments. In between, a transition regime was scheduled. The present study shows the concept of the morphing schedule. The morphing actuator and its capital cost and actuation energy consumption need to be further studied.

To determine a potential morphing schedule of the 25-MW turbine models, the V3 (fixed coning angle) rotor was used as a baseline to determine a morphing version, V3m, which would allow a variable coning angle. The V3 rotor (blade length, mass, etc.) was chosen for the baseline since it is a carefully redesigned model that has enough load margin for morphing operations. To explore the potential morphing schedule space, MATLAB was employed to run FAST while varying the wind speed and the coning angle using the V3 blade. The wind speed ranged from 4 m/s (cut-in) to 24 m/s (cut-out) with 1 m/s bins, and at each given wind speed, the coning angle changed from 2.5° to 75° with 2.5° bins. The parameter space yielded 630 test conditions to consider. Since this is an impractical number of test cases to run with fully turbulent conditions (especially since this may require adapting the controller for many, if not most, of the cases to ensure consistent performance under optimized control), a steady-state inflow approach was considered. A difficult issue when employing steady inflow conditions is that the DEL values for turbulent conditions (usually design drivers) are not known. Therefore, a large safety factor was employed while also maintaining the constraint on 10% of the ultimate values, which is consistently done for the SUMR-13 design [2]. While this is a conservative approach, it is carried out in order to account for uncertainties due to the extreme scales of the turbines.

The morphing schedule was selected based on a series of MATLAB simulations, and the schedule is shown in figure 3. The trade-off is determined by a ratio of loads increase and energy increase. The selected schedule aims to increase AEP and limit mean RFBM. In this schedule, the rotor is opened up to a constant coning angle of 7.5° at low wind speed to capture more energy from the wind, and then the rotor is coned to the designed 22.5° around the rated wind speed. When the wind goes above the rated speed, the coning angle decreases and aligns with the zero-mean RFBM line. More details on determining the morphing schedule can be found in [4].
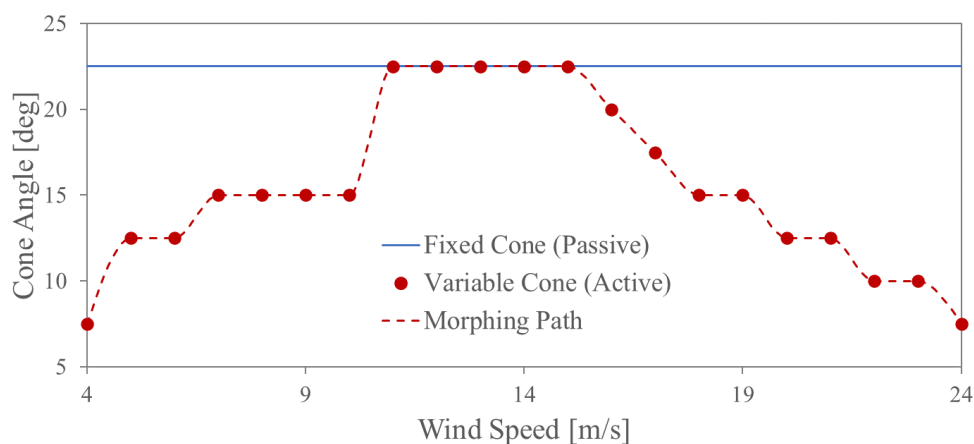

Figure 3. Morphing schedule for active coning V3m rotor (cone angle varies as wind speed changes), compared to the fixed coned V3.
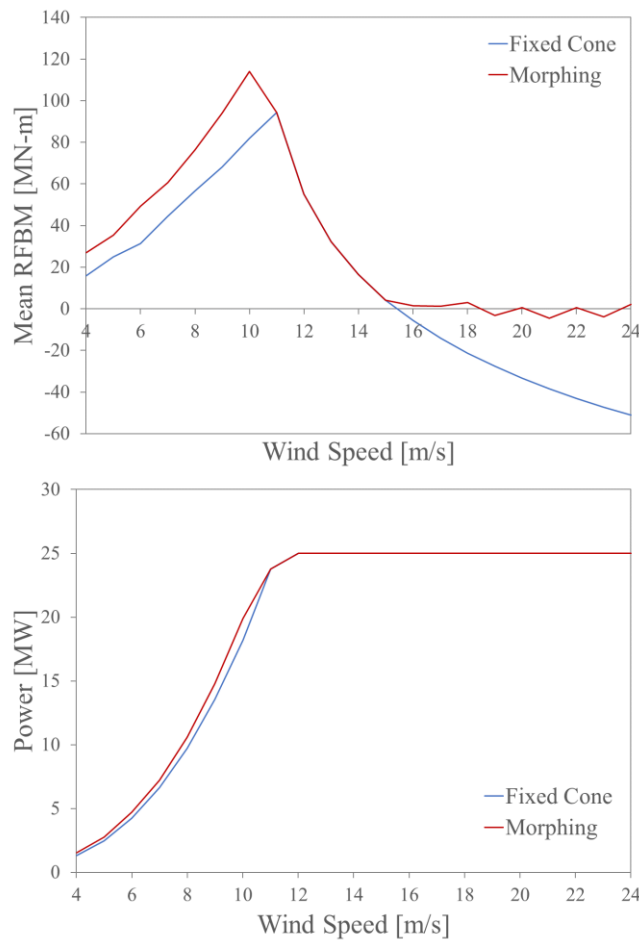
Figure 4. Trade-off between V3 (fixed cone) and V3m (morphing) in
mean root flapwise bending moment (top) and power generation (bottom).

Figure 4 shows the comparison between the fixed coning case (V3) and the active coning case (V3m) with the selected morphing schedule as shown in figure 3. It can be seen that in Region 2 (wind speed below 10 m/s), decreasing cone angles can increase the power output, but the trade-off is that the flapwise MEAN RFBM increases as well. The constraint value for flapwise MEAN is 155 MN-m, and the maximum flapwise bending moment using the morphing schedule does not exceed such a constraint. When the wind speed goes above the rated wind speed of 11.3 m/s, the coning angle decreases and becomes aligned with the zero-mean RFBM, also shown in figure 4.

To consider the AEP output of the wind turbine for a fixed rated power (the generator is held fixed for all these simulations), the capacity factor can be defined as

$$\text{CF} = \left(\sum_{v_{\text{cut-in}}}^{v_{\text{cut-out}}} f_{\text{Weibull}}\left(v_i\right) P_{\text{gen},i} \right) \cdot A \cdot \left(1 - L\right) \Big/ P_{\text{rated}}$$

where $f_{\text{Weibull}}(v_i)$ is the Weibull distribution function (shape factor $k = 2.167$ and scale factor $C = 10.25$ m/s) of a given wind speed v_i and $P_{\text{gen},i}$ is the rated generator power output at the given wind speed v_i. An average availability of 92.2% (A) and an estimated wake loss of $(1-L)$, where L is 9.96%, were assumed; and the result is normalized by the rated wind turbine power $P_{\text{rated}} = 25$ MW. The V3m capacity factor (CF) result for the morphing schedule was further normalized by the CF_0 (i.e., the CF value of V3 equal to 0.44 for the fixed coned baseline rotor). Note that the capital expenditures (CAPEX), balance of system (BOS) costs, and operating expenses (OPEX) are kept the same for both the V3 and V3m systems, so this capacity factor ratio (CF/CF$_0$) is equivalent to (AEP/AEP$_0$), such that a high value of AEP can help minimize LCOE.

The morphing effects have been quantified in AEP and lifetime RFBM damage equivalent load calculations listed in table 2. The V3 model with a fixed coning angle of 22.5° has an AEP of 3,853 MW-hr/MW. As a comparison, the AEP value of the 13.2-MW conventional unconed baseline design is 3,385 MW-hr/MW. The results also show that the primary driver for flapwise and edgewise DELs for the 25-MW rotors is the large fluctuating contribution from the variable loads of thrust and gravity. This large load fluctuation is different from the case of conventional-scale turbines, where turbulent fluctuations are often the primary driver for DELs. Compared with the fixed coned V3 rotor case, the active coning (i.e., morphing) V3m can provide an AEP increase of 6% to 4,090 MW-hr/MW, while the maximum of the mean RFBM across the morphing schedule increases by 21% (still under conservative safety design constraint of 155 MN-m) as a trade-off. Morphing has a negligible effect on the edgewise lifetime DEL, but it can help reduce the maximum edgewise bending moment by 43%. In summary, the aim to limit loads via a larger coned rotor to the levels of the baseline design was successful, and the morphing provides one solution for the extreme-scale rotor to reduce the flapwise loads while maintaining an increase in AEP.

Table 2. Comparisons of MEAN, RMS, and DEL between fixed coned and active coning rotors (in parentheses percent increase or decrease with respect to V3).

	13.2 MW Conventional	25 MW V3	25 MW V3m
AEP [MW-hr/MW]	3,385	3,853 (0%)	4,090 (+6.2%)
Flapwise max MEAN [MN-m] [a]	-	**94.4 (0%)**	**114.1 (+20.9%)**
Flapwise max RMS [MN-m]	-	42.3 (0%)	40.3 (-4.7%)
Flapwise Lifetime DEL [MN-m]	-	58.1 (0%)	49.4 (-15.0%)
Edgewise max MEAN [MN-m]	-	41.3 (0%)	23.7 (-42.6%)
Edgewise max RMS [MN-m]	-	58.3 (0%)	58.3 (0%)
Edgewise Lifetime DEL [MN-m]	-	**114.0 (0%)**	**114.0 (0%)**

[a] **bold** indicates design driving loads

5. Conclusions and Future Work

A series of 25-MW rotor designs was examined at a range of wind speeds in terms of maximum and damage equivalent blade moments and tower-blade clearance. This paper had three main objectives. The first objective was to upscale a 13.2-MW wind turbine system with a downwind two-bladed configuration to a 25-MW design. The second objective was to upgrade the scaled model's aerodynamics, structural design, and controller tuning. The models were successfully developed and simulated with FAST and other codes, and they satisfied the design requirements to operate at high coning angles. Thirdly, the V3 model was employed to integrate morphing to increase the energy capture while limiting the loads. Compared with the fixed coned V3 design, the active coning V3m morphing design can provide a 6% annual energy production increase with the maximum of the blade root flapwise bending moment increasing 21% (still under the safety constraint) as a trade-off. As a result, the series of 25-MW rotors can be a valuable baseline for further development and assessment. The present study is based on steady-state assumptions. In practice, the morphing actuation is going to be very slow, and those actuation and dynamic effects will need to be taken into account in future work, enabling morphing actuation in the simulation codes and validating with IEC standards.

Acknowledgments

References

[1] Zalkind, D.S., Ananda, G.K., Chetan, M., Martin, D.P., Bay, C., Johnson, K.E., Loth, E., Griffith, D.T., Selig, M.S. and Pao, L.Y., 2019. System-level design studies for large rotors. *Wind Energy Science*, Vol. 4, pp. 595-618.

[2] Yao, S., Chetan, M. and Griffith, D.T., 2021. Structural design and optimization of a series of 13.2 MW downwind rotors. *Wind Engineering*, p.0309524X20984164.

[3] Griffith, D.T. and Richards, P.W., 2014. *The SNL100-03 blade: Design studies with flatback airfoils for the Sandia 100-meter blade*. Sandia National Laboratories, SAND2014-18129, Albuquerque, NM.

[4] Qin, C., Loth, E., Zalkind, D.S., Pao, L.Y., Yao, S., Griffith, D.T., Selig, M.S. and Damiani, R., 2020. Downwind coning concept rotor for a 25 MW offshore wind turbine. *Renewable Energy*, 156, pp.314.

[5] Pao, L.Y., Zalkind, D.S., Griffith, D.T., Chetan, M., Selig, M.S., Ananda, G.K., Bay, C.J., Stehly, T. and Loth, E., 2021. Control co-design of 13 MW downwind two-bladed rotors to achieve 25% reduction in levelized cost of wind energy. *Annual Reviews in Control*, Vol. 51, pp. 331-343.

[6] Zalkind, D.S., Dall'Anese, E. and Pao, L.Y., 2020. Automatic controller tuning using a zeroth-order optimization algorithm. *Wind Energy Science*, 5(4), pp.1579-1600.

[7] Jonkman, J., Butterfield, S., Musial, W. and Scott, G., 2009. *Definition of a 5-MW reference wind turbine for offshore system development*. National Renewable Energy Laboratory, NREL/TP-500-38060, Golden, CO.

[8] Zalkind, D.S., Nicotra, M.M. and Pao, L.Y., 2021. Constrained power reference control for wind turbines. *Wind Energy*. DOI: 10.1002/we.2705.

[9] Selig, M.S. and Tangler, J.L., 1995. Development and application of a multipoint inverse design method for horizontal axis wind turbines. *Wind Engineering*, pp. 91-105.

[10] Selig, M. S., PROPID – Software for horizontal-axis wind turbine design and analysis, https://m-selig.ae.illinois.edu/propid.html.

[11] Ananda, G.K., Bansal, S. and Selig, M.S., 2018, Aerodynamic design of a 13.2 MW segmented ultralight morphing rotor. *AIAA SciTech Forum,* AIAA Paper 2018-0994, Kissimmee, FL, January 2018.

[12] Berg, J.C. and Resor, B.R., 2012. *Numerical manufacturing and design tool (NuMAD V2. 0) for wind turbine blades: User's guide.* Sandia National Laboratories, SAND2012-728, Albuquerque, NM.

[13] Bir, G., 2005. *User's guide to BModes (software for computing rotating Beam-coupled Modes)*. National Renewable Energy Laboratory, NREL/TP-500-39133, Golden, CO.

[14] Jonkman, J.M. and Buhl Jr, M.L., 2005. *FAST user's guide.* National Renewable Energy

　　　　　Laboratory, NREL/EL-500-38230, Golden, CO.

[15]　Moriarty, P.J. and Hansen, A.C., 2005. *AeroDyn theory manual*. National Renewable Energy Laboratory, NREL/TP-500-36881, Golden, CO.

[16]　Jonkman, B.J. and Buhl Jr, M.L., 2006. *TurbSim user's guide.* National Renewable Energy Laboratory, NREL/TP-500-39797, Golden, CO.

[17]　Hayman, G.J. and Buhl Jr, M., 2012. *MLife user's guide for version 1.00*. National Renewable Energy Laboratory, Golden, CO.

[18]　Hayman, G., 2012. *MLife theory manual for version 1.00*. National Renewable Energy Laboratory, Golden, CO.

[19]　Ichter, B., Steele, A., Loth, E., Moriarty, P. and Selig, M., 2016. A morphing downwind-aligned rotor concept based on a 13-MW wind turbine. *Wind Energy*, *19*(4), pp. 625-637.